A Distributed Network for Multimodal Experiential Representation of Concepts

Jia-Qing Tong[1,2], Jeffrey R. Binder[1,2], Colin J. Humphries[1], Stephen Mazurchuk[1,2], Lisa L. Conant[1], Leonardo Fernandino[1,3]

[1]Department of Neurology, Medical College of Wisconsin, Milwaukee, WI, USA

[2]Department of Biophysics, Medical College of Wisconsin, Milwaukee, WI, USA

[3]Department of Biomedical Engineering, Medical College of Wisconsin and Marquette University, Milwaukee, WI, USA

Abbreviated title: Multimodal Concept Representation

Corresponding Author:

Leonardo Fernandino, Ph.D.

Departments of Neurology and Biomedical Engineering

Medical College of Wisconsin

8701 W Watertown Plank Rd, Milwaukee, WI 53226

Email: lfernandino@mcw.edu

Office Phone: 414-955-7388

Key words: semantics, concept representation, representational similarity analysis, fMRI

Pages: 33

Figures: 4

Supplementary Tables: 2

Financial interests or conflicts of interest: None.

Acknowledgements:

This work was supported by National Institute on Deafness and Other Communication Disorders (NIDCD) grant R01 DC016622, by the Intelligence Advanced Research Projects Activity under Grant FA8650-14-C-7357, and by a grant from the Advancing a Healthier Wisconsin Foundation (Project #5520462). The authors thank Volkan Arpinar, Elizabeth Awe, Joseph Heffernan, Steven Jankowski, Jedidiah Mathis, and Megan LeDoux for technical assistance.

Abstract

The architecture of the cortical system underlying concept representation is a topic of intense debate. Much evidence supports the claim that concept retrieval selectively engages sensory, motor, and other neural systems involved in the acquisition of the retrieved concept, yet there is also strong evidence for involvement of high-level, supramodal cortical regions. A fundamental question about the organization of this system is whether modality-specific information originating from sensory and motor areas is integrated across multiple "convergence zones" or in a single centralized "hub". We used representational similarity analysis (RSA) of fMRI data to map brain regions where the similarity structure of neural patterns elicited by large sets of concepts matched the similarity structure predicted by a high-dimensional model of concept representation based on sensory, motor, affective, and other modal aspects of experience. Across two studies involving different sets of concepts, different participants, and different tasks, searchlight RSA revealed a distributed, bihemispheric network engaged in multimodal experiential representation, composed of high-level association cortex in anterior, lateral, and ventral temporal lobe; inferior parietal lobule; posterior cingulate gyrus and precuneus; and medial, dorsal, ventrolateral, and orbital prefrontal cortex. These regions closely resemble networks previously implicated in general semantic and "default mode" processing and are known to be high-level hubs for convergence of multimodal processing streams. Supplemented by an exploratory cluster analysis, these results indicate that the concept representation system consists of multiple, hierarchically organized convergence zones supporting multimodal integration of experiential information.

Significance Statement

It has long been known that information about visual, auditory, motor, affective, and other features of our phenomenal experience originate in distinct brain regions. However, it is still unclear how these processing streams converge to form multimodal concept representations.

Using fMRI together with a multimodal experiential model of conceptual content, we show in two large studies that concept knowledge is represented across a distributed, bihemispheric network including temporal, parietal, limbic, and prefrontal association cortices. These results argue against the idea of a single centralized "hub" for concept representation, suggesting instead that multiple high-level convergence zones encode conceptual information in terms of multimodal experiential content.

Introduction

Concepts are the building blocks of meaning and are essential for everyday thinking, planning, and communication, yet there remains considerable debate surrounding their neural implementation. "Grounded" theories of concept representation postulate that sensory-motor and affective representations involved in concept formation are re-activated during concept retrieval (Damasio, 1989; Barsalou, 2008; Glenberg et al., 2009). Support for this claim includes many studies showing that perceptual and motor processing areas are activated when corresponding perceptual or motor information about concepts is retrieved (Meteyard and Vigliocco, 2008; Binder and Desai, 2011; Kiefer and Pulvermuller, 2012; Kemmerer, 2014).

How these multiple modality-specific representations are combined during concept retrieval, however, is not yet clear. Primate cortex contains multiple regions where information converges across sensory modalities (Jones and Powell, 1970; Mesulam, 1998; Man et al., 2013; Man et al., 2015). Portions of the human superior temporal sulcus (STS), for example, are known to respond to tactile, auditory, and visual stimulation (Beauchamp et al., 2008). The homolog of this region in macaque monkeys contains neurons that similarly respond to any of these stimulation modalities (Bruce et al., 1981) and are anatomically connected to corresponding unimodal cortex (Padberg et al., 2003). Other primate brain areas reported to have multimodal characteristics include posterior parietal cortex (Andersen, 1997), prefrontal cortex (Sugihara et al., 2006), parahippocampus (Damasio et al., 1982), and entorhinal cortex

(Van Hoesen et al., 1972). Possible human homologs of these regions include cortical areas identified with the "default mode network", as suggested by a step-wise connectivity analysis of resting-state fMRI (Sepulcre et al., 2012). Beginning with seed regions in multiple primary sensory cortices, these authors showed that connections arising from these regions gradually converge, over multiple connectivity steps, at high-level "hubs" that include much of the lateral temporal cortex, angular gyrus, dorsomedial and inferolateral prefrontal cortex, posterior cingulate gyrus and precuneus.

Various models propose a central role for multimodal or supramodal hubs in concept processing, though both the anatomical location and information content encoded in these hubs remain unclear (Mahon and Caramazza, 2008; Binder and Desai, 2011; Lambon Ralph et al., 2017). One prominent theory proposes that the anterior temporal lobe (ATL) plays a unique role in storing abstract concept representations. During concept retrieval, the central ATL hub would activate modality-specific representations stored in unimodal cortical areas (the "spokes") (Patterson et al., 2007). An alternative model postulates widespread and hierarchically organized convergence zones in multiple brain locations (Damasio, 1989; Mesulam, 1998; Meyer and Damasio, 2009). We have previously proposed that these convergence zones are neurally implemented in the multimodal connectivity hubs identified by Sepulcre et al. (2012), which closely correspond to the regions identified in a large neuroimaging meta-analysis of semantic word processing (Binder et al., 2009). This idea is supported by neuroimaging findings indicating that these cortical regions encode multimodal information about the experiential content of lexical concepts (Bonner et al., 2013; Fernandino et al., 2016b; Fernandino et al., 2016a; Fernandino et al., 2021).

Here we use representational similarity analysis (RSA) with a whole-brain searchlight approach to identify cortical regions involved in multimodal conceptual representation. RSA measures the level of correspondence between the similarity matrix for a set of stimuli (e.g., words) derived from neural data and the similarity matrix for the same stimulus set computed

from an *a priori* representational model (Kriegeskorte et al., 2008). We used a searchlight approach (Kriegeskorte et al., 2008) to generate a map of cortical regions where this representational correspondence holds true. We used an experiential model of conceptual content as the basis for RSA (Binder et al., 2016). Unlike the abstract representations used in previous RSA studies, this model encodes conceptual content explicitly in terms of 65 sensory, motor, affective, and other experiential processes. Identical analyses were run on two large datasets to assess replication across independent participant samples, word sets, and tasks. The analyses provided strong evidence that the multimodal experiential content of lexical concepts is represented across several high-level convergence zones.

Material and Methods

Experiment 1

Participants

Nineteen native English speakers (11 women, 8 men) participated in Experiment 1. Their mean age was 26.4 years (range 20 to 38). All were right-handed according to the Edinburgh handedness inventory (Oldfield, 1971) and had no history of neurological disease. All participants in Experiments 1 and 2 were compensated for their time and gave informed consent in conformity with a protocol approved by the Institutional Review Board of the Medical College of Wisconsin.

Stimuli and Concept Features

The stimuli consisted of 242 words, including 141 nouns, 62 verbs, and 39 adjectives (Supplementary Table 1). The noun concepts included inanimate objects, animate objects, human roles (e.g., mother, doctor), settings (e.g., church, forest), and events. Stimuli were selected by the Intelligence Advanced Research Projects Activity, which funded the study. Experiential representations for these words were available from a previous study in which

ratings on 65 experiential domains were used to represent word meanings in a high-dimensional space (Binder et al., 2016). In brief, the experiential domains were selected based on known neural processing systems – such as color, shape, visual motion, touch, audition, motor control, olfaction – as well as other fundamental aspects of cognition whose neural substrates are less clearly understood, such as space, time, affect, reward, numerosity, and others. Ratings were collected using the crowd sourcing tool Amazon Mechanical Turk, in which volunteers rated the relevance of each experiential domain to a given concept on a 0-6 Likert scale. The value of each feature was represented by averaging ratings across participants. This feature set was highly effective at clustering concepts into traditional taxonomic categories (e.g., animals, plants, vehicles, occupations, etc.) (Binder et al., 2016) and has been used successfully to decode fMRI activation patterns during sentence reading (Anderson et al., 2017; Anderson et al., 2019).

Stimulus Presentation and Tasks

Words were presented visually in a fast event-related procedure with variable inter-stimulus intervals. The entire list was presented to each participant six times in a different pseudorandom order across two separate imaging sessions (3 presentations per session).

Stimuli were presented in white font on a black background. Each trial began with presentation of a single word for 500 ms, followed by a 1.5-sec fixation period (**Figure 1**). Participants were instructed to read each word silently and think about the meaning of the word. To ensure attention to the stimuli, a random 10% of the trials were followed by a semantic-matching probe task, in which 2 words were shown side by side, and the participant indicated by a button press which of the two was more similar in meaning to the word just presented (these probe trials were not included in the analyses). All trials then concluded with presentation of a nonverbal “reset” stimulus for 1.5 seconds, the aim of which was to suppress processing of the previously presented word. The reset stimulus consisted of two grey squares presented side by

side and separated by a vertical black line. The participant indicated by a button press which of the two squares was brighter. A variable fixation period of 0-4 sec followed all trials prior to the beginning of the next trial.

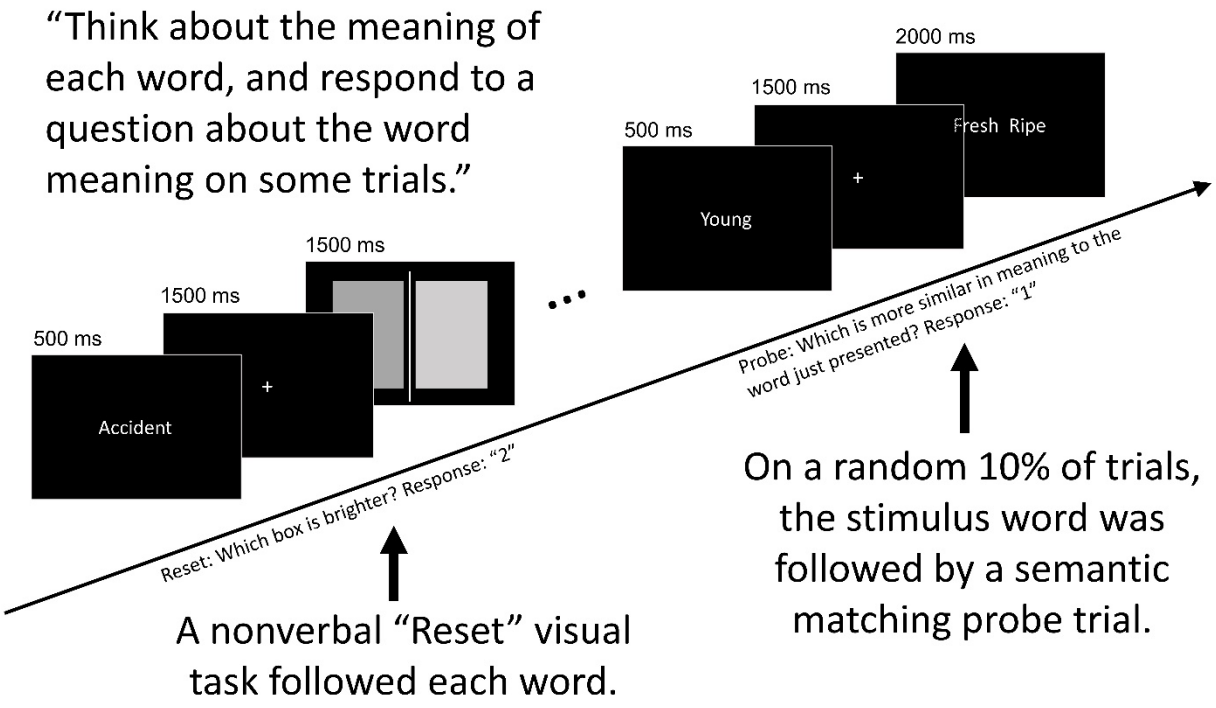

Figure 1. Schematic illustration of the tasks used in Experiment 1.

Each presentation of 242 test words and 26 probe trials (268 trials in total) occurred over the course of four imaging runs, each lasting 6 minutes. The four runs that comprised one repeat of the entire list was referred to as a "set". To minimize lexical ambiguity, grammatical class was used to block items by run. This was necessary because many of the nouns in the list can also be used as verbs, and several had very different semantic features when used as nouns vs. verbs (e.g., 'left', 'duck', 'saw', 'fence', 'spring'). Although the verbs in the set were all in past tense, several are also used commonly as adjectival participles ('celebrated', 'damaged', 'lost', 'planned', 'used'). Thus, nouns and verbs were presented in different runs, and adjectives

were blocked with the nouns to separate them from the verbs. The nouns and adjectives were distributed evenly across 3 of the 4 imaging runs in each set, with the runs balanced on word class and noun category. Each of these 3 runs thus included 13 adjectives, 4-5 event nouns, 8 animate object nouns, 12-13 inanimate object nouns, 12-13 human role nouns, and 10 setting nouns. The remaining run of each set contained all 62 verbs.

Stimuli for probe trials were selected pseudo-randomly with replacement. For the 3 noun-adjective runs, a random set of either 6 or 7 probe trial words was selected for each run from the words comprising the other two noun-adjective runs, such that no stimulus used on a probe trial was repeated within the same run. This was not possible for the verb run, since all 62 verbs were presented in the same run. Thus, for the verb run, 7 verbs appeared twice – one time followed by a probe and one time without a probe.

Nine complete sets were composed in this way. Six were selected for each participant, with counterbalancing across participants. In addition, the order of presentation within each run was randomized for each participant to eliminate order effects at the group level.

MRI Data Acquisition and Processing

Images were acquired with a 3T GE 750 scanner at the Center for Imaging Research of the Medical College of Wisconsin. High-resolution T1-weighted anatomical images were acquired with a 3D spoiled gradient echo sequence (FOV = 240 mm, 220 axial slices, in-plane matrix = 256 x 224, voxel size = 1 x 1 x 1 mm^3). T2-weighted anatomical images were acquired with a CUBE T2 sequence (FOV = 256 mm, 168 sagittal slices, in-plane matrix = 256 x 256, voxel size = 1 x 1 x 1 mm^3). T2*-weighted gradient-echo echoplanar images were obtained for functional imaging (TR = 2000 ms, TE = 24 ms, flip angle = 77°, FOV = 192 mm, 41 axial slices, in-plane matrix = 64 x 64, voxel size = 3 x 3 x 3 mm^3).

Preprocessing was performed using AFNI. EPI images were corrected for slice timing. All images were then aligned to the 3rd functional image in the series before aligning to the T1-

weighted anatomical image. All voxels were normalized to have a mean of 100 and a range of 0 to 200. A general linear model was built to fit the time series of the functional data via multivariable regression. Each word was treated as a single regressor of interest, which included the 6 repetitions of the word and excluded any probe task trials involving that word, resulting in 242 beta coefficient maps. Regressors of no interest included 12 degrees of freedom of head motion, response time for the reset task, and response time for the probe task trials. Individual word, reset, and probe task event regressors were convolved with a hemodynamic response function. A *t* statistical map was generated for each word and these maps were subsequently used for the searchlight RSA.

Surface-Based Searchlight Representational Similarity Analysis

To optimize alignment between participants and to constrain the searchlight analysis to cortical grey matter, individual brain surface models were constructed from T1-weighted and T2-weighted anatomical data using Freesurfer and the HCP pipeline (Glasser et al., 2013). The cortex ribbon was reconstructed in standard grayordinate space with 2-mm spaced vertices. We visually checked the quality of reconstructed surfaces before carrying out the analysis. Segmentation errors were corrected manually, and the corrected images were fed back to the pipeline to produce the final surfaces. Only cortical grey matter was included in the analysis.

RSA was carried out using custom Python and Matlab scripts. Searchlight RSA typically employs spherical volumes moved systematically through the brain or the cortical grey matter voxels. This method, however, does not exclude signals from white matter voxels that happen to fall within the sphere, and which may contribute noise. Spherical volumes may also erroneously combine non-contiguous cortical regions across sulci. Surface-based searchlight analysis overcomes these shortcomings using circular 2-dimensional “patches” confined to contiguous vertices on the cortical surface. At each vertex, a fast-marching algorithm was applied to create a 5-mm radius patch around the seed vertex on the midthickness surface, resulting in a group of

vertices comprising each patch. These vertices were then mapped one by one back to the native volume space of the participant to label voxels associated with the surface patch. To avoid partial-volume effects, we included only voxels that contained the entire middle 80% of the cortical ribbon at the mapped vertex location. Each surface vertex was thus associated with a group of voxels in native space (the searchlight ROI) for subsequent RSA.

Representational dissimilarity matrices (RDMs) were calculated for the semantic model (the model RDM) and for each vertex-associated ROI (the neural RDM). Each entry in the neural RDM represented the correlation distance between fMRI responses evoked by two different words. Neural RDMs were computed for each of the 64,984 vertices. For the model RDM, we calculated the cosine distances between each pair of words in the 65-dimensional experiential feature space. A word length RDM, created by taking the absolute difference in letter length between each word pair, was included as a covariate matrix of no interest. Pearson correlations between neural RDMs and the model RDM were computed controlling for the word length RDM, resulting in a partial correlation score map on the surface for each participant.

Finally, second level analysis was performed on the partial correlation score maps after alignment of each individual map to a common surface template (generated by averaging the individual 32k_FS_LR meshes produced by the HCP pipeline), Fisher z-transformation, and smoothing of the maps with a 6-mm full width at half maximum Gaussian kernel. A one-tailed, one-sample t-test against zero was applied at all vertices. FSL's PALM was used for non-parametric permutation testing to determine cluster-level statistical inference. Cluster-level statistical inference was implemented with a cluster-forming threshold of $z > 3.1$ ($p < 0.001$). The distribution of the largest clusters across permutations, in which the correlations were randomly sign-flipped 10,000 times, was calculated, and a significance level of $\alpha < 0.01$ was set. The final data were rendered on the group averaged HCP template surface.

Experiment 2

Participants

Experiment 2 involved 22 right-handed, native English speakers (11 women, 11 men; mean age 29.1; range 20 to 41). None of the participants took part in Experiment 1. This dataset was reported in a previous study (Fernandino et al., 2021).

Stimuli

Stimuli (see Supplementary Table 2) included 160 object nouns (40 each of animals, foods, tools, and vehicles) and 160 event nouns (40 each of social events, verbal events, non-verbal sound events, and negative events). Of the 320 concepts included in Experiment 2, 24 objects and 9 events were also used in Experiment 1. Concept ratings on the same 65 experiential domains used for the model in Experiment 1 were obtained for each concept using the same crowd-sourcing methods as in Experiment 1.

Stimulus Presentation and Tasks

As in Experiment 1, words were presented visually in a fast event-related procedure with variable inter-stimulus intervals, and the entire list was presented 6 times in random order over three imaging sessions performed on separate days.

On each trial, a noun was displayed in white font on a black background for 500 ms, followed by a 2.5-second blank screen. Each trial was followed by a central fixation cross with variable duration between 1 and 3 s (mean = 1.5 s). Participants rated each noun according to how often they encountered the corresponding entity or event in their daily lives, on a scale from 1 (“rarely or never”) to 3 (“often”). This familiarity judgment task was designed to encourage semantic processing of the word stimuli without emphasizing any particular semantic features or dimensions. Participants indicated their response by pressing one of three buttons on a response pad with their right hand. In contrast to Experiment 1, no reset task was used.

Each presentation of the 320 test words occurred over the course of 4 imaging runs. Each session consisted of 2 presentations of the full list (8 runs).

MRI Data Acquisition and Processing

Images were acquired with a 3T GE Premier scanner at the Medical College of Wisconsin. Structural imaging included a T1-weighted MPRAGE volume (FOV = 256 mm, 222 axial slices, voxel size = 0.8 x 0.8 x 0.8 mm^3) and a T2-weighted CUBE acquisition (FOV = 256 mm, 222 sagittal slices, voxel size = 0.8 x 0.8 x 0.8 mm^3). T2*-weighted gradient-echo echoplanar images were obtained for functional imaging using a simultaneous multi-slice sequence (SMS factor = 4, TR = 1500 ms, TE = 23 ms, flip angle = 50°, FOV = 208 mm, 72 axial slices, in-plane matrix = 104 x 104, voxel size = 2 x 2 x 2 mm^3). A pair of T2-weighted spin echo echo-planar scans (5 volumes each) with opposing phase-encoding directions was acquired before run 1, between runs 4 and 5, and after run 8, to provide estimates of EPI geometric distortion in the phase-encoding direction due to B0 inhomogeneities.

In addition to the preprocessing steps described above for Experiment 1, functional images were also corrected for geometric distortion using AFNI's 3dQwarp, which implemented non-linear transformations estimated from the paired T2-weighted spin echo images. As in Experiment 1, each word was treated as a single regressor of interest and convolved with a hemodynamic response function, resulting in 320 beta coefficient maps. Head motion vectors were again included as regressors of no interest. Response time z-score on each trial of the familiarity judgment task was also included as a covariate of no interest.

Surface-Based Searchlight Representational Similarity Analysis

RSA analysis, generation of group maps, and thresholding methods for Experiment 2 were identical to those used for Experiment 1.

320 **Hierarchical clustering based on neural similarity structure**

321 Although the regions identified in Experiments 1 and 2 all show neural similarity structures that
322 are correlated with the semantic model structure, it is possible that they vary somewhat in their
323 information content. To investigate relative differences and similarities between the
324 representational structure of the various regions identified in the RSAs, we performed
325 hierarchical clustering analysis on the *neural* RDMs of these regions, as follows. First, the group
326 maps from each experiment were thresholded at $p < .0005$ to separate minimally connected
327 regions and highlight vertices with strong correlations to the semantic model. These maps were
328 then overlapped to identify vertices common to both experiments. These steps resulted in 23
329 regions common to both analyses, which were used as regions of interest (ROIs) for the
330 hierarchical clustering analysis. At the individual participant level, within each ROI, seed vertices
331 with the highest correlation scores were combined iteratively until a set of approximately 100
332 voxels associated with these vertices was compiled. A neural RDM was then computed for each
333 such voxel set, resulting in 23 RDMs for each individual. Pairwise RDM correlation was
334 calculated for these 23 voxel sets at the individual level, resulting in a new 23 x 23 matrix in
335 which each entry represented the correlation between neural RDMs of two ROIs. These
336 matrices were then averaged across all 41 participants, and hierarchical clustering was
337 implemented on this averaged matrix, excluding the diagonal. Ward's variance minimization
338 algorithm was applied to calculate distances between clusters.
339
340 **Results**
341 **Experiment 1.** "Probe" trials requiring semantic forced-choice matching of 2 words with the
342 preceding list word were presented after 10% of list words to encourage attention to the list
343 words. One participant failed to provide responses on this task, probably due to inadequate
344 instruction. For the remaining participants, the mean response rate was 95.5% (SD 4.2%), and
345 mean accuracy was 82.1% (SD 7.0%). A perceptual "reset" task occurred after all list words

(and probe trials) with the aim of curtailing processing of the previous list word. The mean response rate on this task was 98.9% (SD 2.5%), and mean accuracy was 96.1% (SD 4.6%).

Group-level searchlight RSA showed a bilateral, distributed network of regions where neural similarity correlated with semantic similarity across the 242 list words (**Figure 2, left**). Extensive temporal lobe involvement included much of the temporal pole, superior temporal sulcus (STS) and middle temporal gyrus (MTG), and anterior fusiform and parahippocampal gyri bilaterally. The inferior temporal gyrus (ITG) was also involved, more so on the left. Parietal lobe involvement was mainly in the inferior parietal lobule, including angular and supramarginal gyri (AG and SMG) bilaterally. Frontal lobe regions included the inferior frontal gyrus (IFG), much of the superior frontal gyrus (SFG) laterally and medially, more restricted patches in the middle frontal gyrus, and orbital frontal cortex bilaterally. Small regions of the precentral gyrus were involved in both hemispheres, and there was substantial involvement of the right insula. On the medial surface there was extensive involvement of the posterior cingulate gyrus and adjacent precuneus bilaterally, and the rostral anterior cingulate cortex bilaterally.

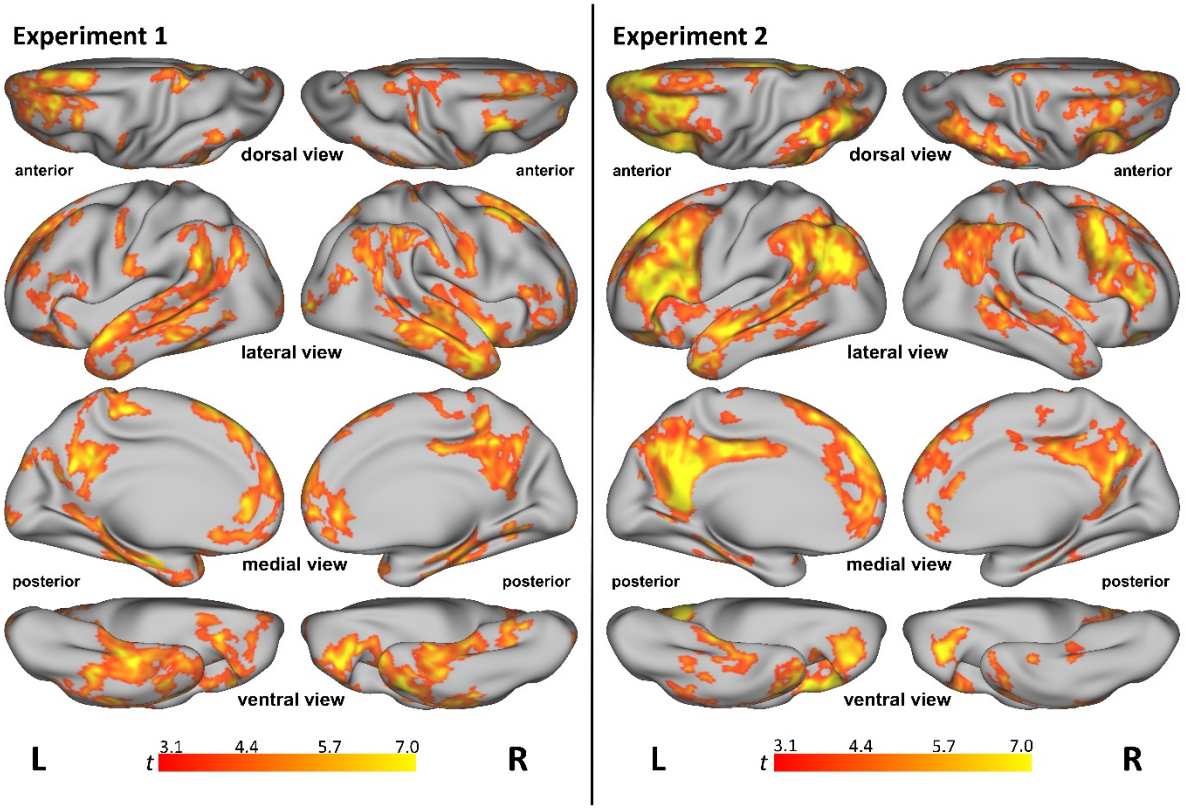

Figure 2. Brain areas where similarity between the neural patterns evoked by concepts was significantly correlated with concept similarity according to the semantic model. Results for Experiment 1 (left) and Experiment 2 (right) are shown on dorsal, lateral, medial, and ventral surface views. All results are significant at $p < 0.001$ and cluster corrected at $\alpha < 0.01$. Colors represent t values.

Experiment 2. The mean response rate on the familiarity judgment task was 98.6% (SD 2.3%). Intra-individual consistency in familiarity ratings across the 6 repetitions of each word was evaluated using intraclass correlations (ICCs) based on a single measurement, two-way mixed effects model and the absolute agreement definition. Results suggested generally good overall intra-individual agreement, with individual ICCs ranging from fair to excellent (mean ICC = 0.661, range: 0.438 – 0.858, all *p*s<0.00001) (Cicchetti, 1994). To examine consistency in

familiarity ratings across participants, responses to the 6 repetitions were first averaged within individuals, and the ICC across participants was calculated using the consistency definition. The resulting ICC of 0.595 (95% confidence interval [0.556, 0.635], $p < .00001$) suggested fair to good inter-individual consistency.

As with Experiment 1, group-level searchlight RSA showed a bilateral, distributed network of regions where neural similarity correlated with semantic similarity across the test concepts (**Figure 1, right**). Most of these overlapped with those in Experiment 1, including temporal pole, STS, MTG, AG, SMG, IFG, SFG, and posterior cingulate/precuneus (PCC) bilaterally. Compared to Experiment 1, there was notably more extensive involvement of lateral prefrontal cortex, including inferior and middle frontal gyri, bilaterally, and somewhat less extensive ventral temporal lobe involvement. Areas of overlap between the two experiments are shown in **Figure 3**.

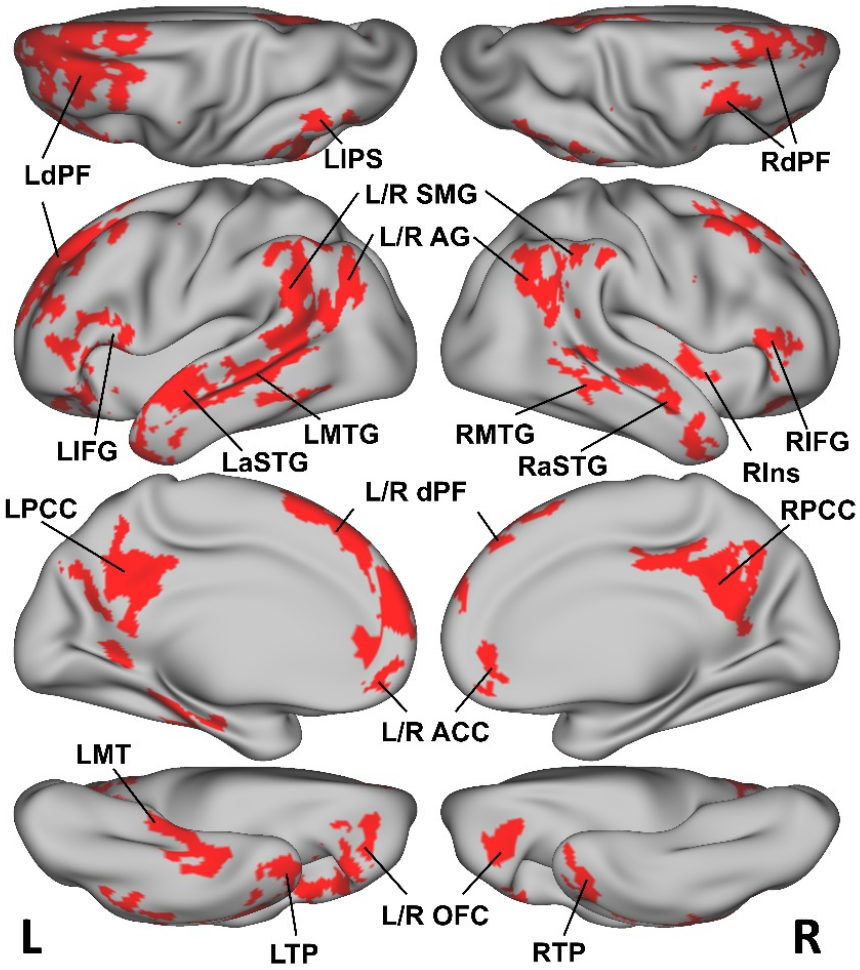

Figure 3. Brain areas where neural similarity was significantly correlated with model similarity in both Experiment 1 and Experiment 2. LACC: left anterior cingulate cortex; LAG: left angular gyrus; LaSTG: left anterior superior temporal gyrus; LdPF: left dorsal prefrontal cortex; LIFG: left inferior frontal gyrus; LIPS: left intraparietal sulcus; LMT: left medial temporal lobe; LMTG: left middle temporal gyrus; LOFC: left orbital frontal cortex; LPCC: left posterior cingulate and precuneus cortex; LSMG: left supramarginal gyrus; LTP: left temporal pole; RAG: right angular gyrus; RaSTG: right anterior superior temporal gyrus; RdPF: right dorsal prefrontal cortex; RIFG: right inferior frontal gyrus; RIns: right insula; RMT: right medial temporal lobe; RMTG: right middle temporal gyrus; ROFC: right orbital frontal cortex; RPCC: right posterior cingulate and precuneus cortex; RSMG: right supramarginal gyrus; RTP: right temporal pole.

Hierarchical clustering of neural similarity structures. Overlap of the Experiment 1 and Experiment 2 RSA maps showed 23 regions common to both (color-coded in **Figure 4, right**). Degree of similarity between the neural RDMs extracted from each of these regions was examined using hierarchical cluster analysis (**Figure 4, left**). The results revealed a division between ROIs in the parietal lobe (PCC, AG, SMG, left intraparietal sulcus) and lateral temporal lobe in one major cluster, and ROIs in the medial temporal lobe, temporal pole, and frontal lobes in another major cluster. The parietal/lateral temporal cluster was further divided by hemisphere, such that right AG, SMG, MTG, and anterior STG fell in one subcluster, and left parietotemporal ROIs in another, along with left and right PCC. The other main cluster included a "limbic" subcluster consisting of bilateral temporal poles, parahippocampus/hippocampus, and right insula. A final subcluster included all frontal lobe ROIs and the left anterior STG.

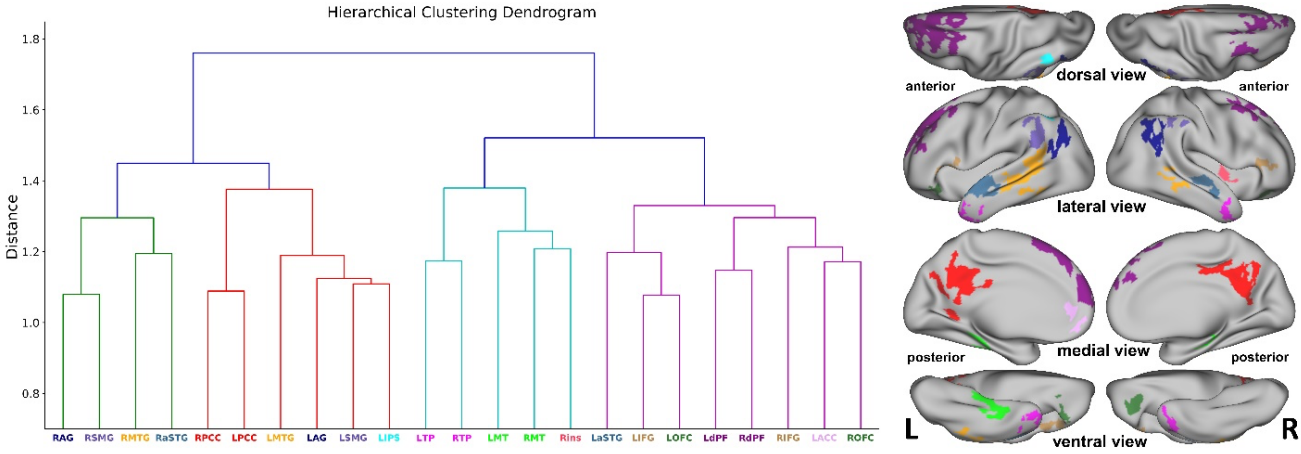

Figure 4. Results of hierarchical clustering of neural similarity structures. Left: Dendrogram based on the averaged similarity structures of neural data from 23 ROIs. The vertical axis indicates linkage distance. Right: The 23 ROIs defined by overlapping the RSA maps from the

two experiments after thresholding each map at $p < 0.0005$ and cluster-correcting at $\alpha < 0.01$. Anatomical labels match those in Figure 3.

Discussion

We sought to clarify the large-scale architecture of the concept representation system by identifying cortical regions whose activation patterns encoded multimodal experiential information about individual lexical concepts. Previous whole-brain searchlight RSA studies on this topic have used semantic representation models based on category membership, semantic feature lists, or word co-occurrence statistics, producing highly variable results. Here we used a model based entirely on multimodal experiential content with no explicit reference to taxonomic or distributional similarity. Across two independent experiments, each involving a large number and a wide range of concepts, we detected multimodal concept representation in widespread heteromodal cortical regions, bilaterally, including anterior and posterior temporal cortex, inferior parietal cortex, posterior cingulate gyrus and precuneus, and medial, dorsal, ventrolateral, and ventral prefrontal regions. These results call into question the idea that information streams originating in unimodal cortical areas are integrated at a single anatomically localized hub for concept representation.

Four previous RSA studies using semantic models and word stimuli implicated anteromedial temporal cortex, particularly perirhinal cortex, as a semantic hub (Devereux et al., 2013; Liuzzi et al., 2015; Martin et al., 2018; Liuzzi et al., 2019). All used semantic models based on crowd-sourced feature production lists, and all used a feature verification task during fMRI (e.g., “WASP – Does it have paws?”). Validity issues with feature production lists have been noted previously, such as the fact that many features people produce are multimodal or highly abstract, and some types of features are difficult to verbalize or systematically ignored (Hoffman and Lambon Ralph, 2013). Another potential problem with these RSA studies is that the verification task used during fMRI requires semantic processing of the explicitly named

448 feature, which logically must contribute to the observed neural activation pattern but is not
449 coded in the semantic model. These problems may have weakened the ability of these studies
450 to detect other regions involved in concept representation.

451 Prior studies combining searchlight RSA with either taxonomic (Devereux et al., 2013;
452 Carota et al., 2021) or distributional (Anderson et al., 2015; Carota et al., 2021) semantic
453 models have implicated more widespread regions, including posterior lateral temporal cortex,
454 inferior parietal lobe, posterior cingulate gyrus, and prefrontal cortex. Only one of these studies
455 (Anderson et al., 2015) reported any representational correspondence in medial or ventral
456 temporal areas. The two studies using taxonomic models (Devereux et al., 2013; Carota et al.,
457 2021) showed similar involvement of the left posterior superior temporal sulcus and MTG, with
458 extension into adjacent AG and SMG. In contrast, the two studies using distributional models
459 (Anderson et al., 2015; Carota et al., 2021) found little or no posterior temporal involvement, and
460 inferior parietal involvement was confined mainly to the left SMG. Frontal cortex involvement
461 was uniformly present but highly variable in extent and location across the studies. Two studies
462 reported involvement of the posterior cingulate/precuneus (Devereux et al., 2013; Anderson et
463 al., 2015).

464 Several factors may have negatively impacted sensitivity and reliability in these studies.
465 First, ROI-based RSAs show that, relative to experiential models of concept representation,
466 taxonomic and distributional models are consistently less sensitive to the neural similarity
467 structure of lexical concepts (Fernandino et al., 2021). Furthermore, most of the prior studies
468 used volume-based spherical searchlights, which typically sample a mix of grey and white
469 matter voxels, while the surface-based approach used in the present study ensures that only
470 contiguous cortical gray matter voxels are included, thus reducing noise from uninformative
471 voxels. Finally, the nature of the task and the particularities of the concept set used as stimuli
472 can affect both the sensitivity of the analysis and the cortical distribution of the RSA searchlight
473 map, and variations in these properties may underlie some of the variation in results across

474 studies. We dealt with this issue by (1) employing large numbers of concepts from diverse
475 semantic categories and (2) by analyzing data from two independent experiments to identify
476 areas displaying reliable representational correspondence with the semantic model across
477 different concept sets and different tasks.

478 The network of brain regions identified in the current study closely resembles the
479 network identified previously in a meta-analysis of 120 functional imaging studies on semantic
480 processing (Binder et al., 2009). The results provide novel evidence that these brain regions,
481 consisting essentially of heteromodal association areas distant from primary sensory and motor
482 systems, represent conceptual information in terms of multimodal experiential content. In
483 contrast to previous RSA studies of concept representation (Devereux et al., 2013; Anderson et
484 al., 2015; Martin et al., 2018; Carota et al., 2021), the network includes extensive cortex in the
485 ATL, a region strongly implicated in high-level semantic representation (Lambon Ralph et al.,
486 2017). Although the current results support a role for the ATL in concept representation, they
487 argue against it having a unique role as a central integration hub.

488 The concept representation network identified in the current study also closely
489 resembles the set of brain regions referred to as the "default mode network" (Buckner et al.,
490 2008). This overlap supports the view that concept retrieval and manipulation are major
491 components of the brain's "default mode" of processing (Binder et al., 1999; Binder et al., 2009;
492 Andrews-Hanna et al., 2014). Our results add to prior evidence by showing that the
493 representational structure of neural activity in these regions reflects the experiential content of
494 lexical concepts.

495 The finding of extensive frontal lobe involvement in concept "representation" deserves
496 comment. Studies of brain damaged individuals and functional imaging experiments in the
497 healthy brain have long been interpreted as supporting the classic view that frontal cortex plays
498 an operational control rather than an information storage function in the brain (Stuss and
499 Benson, 1986; Kimberg and Farah, 1993; Thompson-Schill et al., 1997; Wagner et al., 2001).

Nevertheless, nearly all RSA studies of concept representation have observed similarity structure correlations in prefrontal regions. Why would activity in these areas reflect semantic content? We believe these observations can be reconciled with the classic view by postulating a more fine-grained organization of control systems in the frontal lobe than is usually assumed in semantic theories. Rather than being composed of large, homogeneous areas with a nonspecific control function, control systems in the prefrontal cortex may be tuned, at a relatively small scale, to particular sensory-motor and affective features. Neurophysiological studies in nonhuman primates provide evidence for tuning of prefrontal neurons to preferred stimulus modalities (Romanski, 2007), as well as differential connectivity across the prefrontal cortex with various sensory systems (Barbas and Mesulam, 1981; Petrides, 2005). A few human functional imaging studies provide similar evidence for sensory modality tuning in prefrontal cortex (Greenberg et al., 2010; Michalka et al., 2015; Tobyne et al., 2017). If conceptual representation in temporal and parietal cortex is inherently organized according to experiential content, it seems plausible that controlled activation and short-term maintenance of this information would require similarly fine-grained control mechanisms.

This hypothesis finds some support in a comparison of our two experiments. The infrequent probe task procedure used in Experiment 1 was intentionally designed to minimize explicit, goal-directed retrieval of semantic information, and the inclusion of a non-semantic perceptual discrimination task after each trial likely encouraged participants to focus their attention on this task rather than on semantic retrieval. In contrast, the task in Experiment 2 required participants to make a semantic decision about each word. Compared to Experiment 1, the Experiment 2 results show much more extensive involvement of lateral prefrontal cortex. A likely interpretation is that the explicit task in Experiment 2 led to stronger engagement of feature-specific control networks in these frontal regions. We propose that the information represented in these prefrontal regions reflects their entrainment to experiential representations

525 stored primarily in temporoparietal cortex, providing context-dependent control over their level of
526 activation.

527 Related to this issue is the question of how similar the many regions identified by RSA
528 are to each other in terms of their representational structure. Although RSA ensures that the
529 neural similarity structure of all these regions is related to the similarity structure encoded in the
530 semantic model, representational structure should be expected to vary to some degree across
531 distinct functional regions. An exploratory cluster analysis of the neural RDMs from these
532 regions suggests a broad distinction between two clusters, one consisting of medial and lateral
533 parietal cortex and posterior lateral temporal areas (across both hemispheres) and the other
534 consisting of medial, ventral, and anterior temporal areas, right insula, and frontal areas. There
535 was also evidence for a distinction between left and right parietotemporal representational
536 structures. These results are consistent with proposed distinctions between the functions of
537 frontal, posterior association, and limbic cortices, as well as longstanding claims regarding
538 interhemispheric differences in semantic representation (Beeman and Chiarello, 1998).
539 Interestingly, this analysis suggests that representations in the ATL are more similar to those in
540 prefrontal areas than to those in posterior temporal and parietal areas involved in the
541 representation of objects and events (Martin, 2007; Bedny et al., 2014). More research is
542 needed to understand the factors that underlie these regional differences in representational
543 content.
544

References

Andersen RA (1997) Multimodal integration for the representation of space in the posterior parietal cortex. Philos Trans R Soc Lond B Biol Sci 352:1421-1428.

Anderson AJ, Bruni E, Lopopolo A, Poesio M, Baroni M (2015) Reading visually embodied meaning from the brain: Visually grounded computational models decode visual-object mental imagery induced by written text. Neuroimage 120:309-322.

Anderson AJ, Binder JR, Fernandino L, Humphries CJ, Conant LL, Raizada RDS, Lin F, Lalor EC (2019) An integrated neural decoder of linguistic and experiential meaning. J Neurosci 39:8969-8987.

Anderson AJ, Binder JR, Fernandino L, Humphries CJ, Conant LL, Aguilar M, Wang X, Doko D, Raizada RDS (2017) Predicting neural activity patterns associated with sentences using a neurobiologically motivated model of semantic representation. Cereb Cortex 27:4379-4395.

Andrews-Hanna JR, Smallwood J, Spreng RN (2014) The default network and self-generated thought: Component processes, dynamic control, and clinical relevance. Ann N Y Acad Sci 1316:29-52.

Barbas H, Mesulam MM (1981) Organization of afferent input to subdivisions of area 8 in the rhesus monkey. J Comp Neurol 200:407-431.

Barsalou LW (2008) Grounded cognition. Annu Rev Psychol 59:617-645.

Beauchamp MS, Yasar NE, Frye RE, Ro T (2008) Touch, sound and vision in human superior temporal sulcus. Neuroimage 41:1011-1020.

Bedny M, Dravida S, Saxe R (2014) Shindigs, brunches, and rodeos: The neural basis of event words. Cogn Affect Behav Neurosci 14:891-901.

Beeman M, Chiarello C (1998) Right hemisphere language comprehension: Perspectives from cognitive neuroscience: Psychology Press.

Binder JR, Desai RH (2011) The neurobiology of semantic memory. Trends Cogn Sci 15:527-536.

568 Binder JR, Desai RH, Graves WW, Conant LL (2009) Where is the semantic system? A critical review and
569 meta-analysis of 120 functional neuroimaging studies. Cereb Cortex 19:2767-2796.
570 Binder JR, Frost JA, Hammeke TA, Bellgowan PS, Rao SM, Cox RW (1999) Conceptual processing during
571 the conscious resting state. A functional MRI study. J Cogn Neurosci 11:80-95.
572 Binder JR, Conant LL, Humphries CJ, Fernandino L, Simons SB, Aguilar M, Desai RH (2016) Toward a
573 brain-based componential semantic representation. Cogn Neuropsychol 33:130-174.
574 Bonner MF, Peelle JE, Cook PA, Grossman M (2013) Heteromodal conceptual processing in the angular
575 gyrus. Neuroimage 71:175-186.
576 Bruce C, Desimone R, Gross CG (1981) Visual properties of neurons in a polysensory area in superior
577 temporal sulcus of the macaque. J Neurophysiol 46:369-384.
578 Buckner RL, Andrews-Hanna JR, Schacter DL (2008) The brain's default network: Anatomy, function, and
579 relevance to disease. Ann N Y Acad Sci 1124:1-38.
580 Carota F, Nili H, Pulvermuller F, Kriegeskorte N (2021) Distinct fronto-temporal substrates of
581 distributional and taxonomic similarity among words: Evidence from rsa of bold signals.
582 Neuroimage 224:117408.
583 Damasio AR (1989) Time-locked multiregional retroactivation: A systems-level proposal for the neural
584 substrates of recall and recognition. Cognition 33:25-62.
585 Damasio AR, Damasio H, Van Hoesen GW (1982) Prosopagnosia: Anatomic basis and behavioral
586 mechanisms. Neurology 32:331-341.
587 Devereux BJ, Clarke A, Marouchos A, Tyler LK (2013) Representational similarity analysis reveals
588 commonalities and differences in the semantic processing of words and objects. J Neurosci
589 33:18906-18916.
590 Fernandino L, Conant LL, Humphries CJ, Binder JR (2021) Decoding the information structure underlying
591 the neural representation of concepts. bioRxiv:2021.2003.2016.435524.

592 Fernandino L, Humphries CJ, Conant LL, Seidenberg MS, Binder JR (2016a) Heteromodal cortical areas
593 encode sensory-motor features of word meaning. J Neurosci 36:9763-9769.
594 Fernandino L, Binder JR, Desai RH, Pendl SL, Humphries CJ, Gross WL, Conant LL, Seidenberg MS (2016b)
595 Concept representation reflects multimodal abstraction: A framework for embodied semantics.
596 Cereb Cortex 26:2018-2034.
597 Glasser MF, Sotiropoulos SN, Wilson JA, Coalson TS, Fischl B, Andersson JL, Xu J, Jbabdi S, Webster M,
598 Polimeni JR, Van Essen DC, Jenkinson M, Consortium WU-MH (2013) The minimal preprocessing
599 pipelines for the human connectome project. Neuroimage 80:105-124.
600 Glenberg AM, Webster BJ, Mouilso E, Havas D, Lindeman LM (2009) Gender, emotion, and the
601 embodiment of language comprehension. 1:151-161.
602 Greenberg AS, Esterman M, Wilson D, Serences JT, Yantis S (2010) Control of spatial and feature-based
603 attention in frontoparietal cortex. J Neurosci 30:14330-14339.
604 Hoffman P, Lambon Ralph MA (2013) Shapes, scents and sounds: Quantifying the full multi-sensory basis
605 of conceptual knowledge. Neuropsychologia 51:14-25.
606 Jones EG, Powell TP (1970) An anatomical study of converging sensory pathways within the cerebral
607 cortex of the monkey. Brain 93:793-820.
608 Kemmerer DL (2014) Cognitive neuroscience of language. New York, NY: Psychology Press.
609 Kiefer M, Pulvermuller F (2012) Conceptual representations in mind and brain: Theoretical
610 developments, current evidence and future directions. Cortex 48:805-825.
611 Kimberg DY, Farah MJ (1993) A unified account of cognitive impairments following frontal lobe damage:
612 The role of working memory in complex, organized behavior. J Exp Psychol Gen 122:411-428.
613 Kriegeskorte N, Mur M, Bandettini P (2008) Representational similarity analysis - connecting the
614 branches of systems neuroscience. Front Syst Neurosci 2:4.

615 Lambon Ralph MA, Jefferies E, Patterson K, Rogers TT (2017) The neural and computational bases of
616 semantic cognition. Nat Rev Neurosci 18:42-55.
617 Liuzzi AG, Dupont P, Peeters R, Bruffaerts R, De Deyne S, Storms G, Vandenberghe R (2019) Left
618 perirhinal cortex codes for semantic similarity between written words defined from cued word
619 association. Neuroimage 191:127-139.
620 Liuzzi AG, Bruffaerts R, Dupont P, Adamczuk K, Peeters R, De Deyne S, Storms G, Vandenberghe R (2015)
621 Left perirhinal cortex codes for similarity in meaning between written words: Comparison with
622 auditory word input. Neuropsychologia 76:4-16.
623 Mahon BZ, Caramazza A (2008) A critical look at the embodied cognition hypothesis and a new proposal
624 for grounding conceptual content. J Physiol Paris 102:59-70.
625 Man K, Kaplan J, Damasio H, Damasio A (2013) Neural convergence and divergence in the mammalian
626 cerebral cortex: From experimental neuroanatomy to functional neuroimaging. J Comp Neurol
627 521:4097-4111.
628 Man K, Damasio A, Meyer K, Kaplan JT (2015) Convergent and invariant object representations for sight,
629 sound, and touch. Hum Brain Mapp 36:3629-3640.
630 Martin A (2007) The representation of object concepts in the brain. Annu Rev Psychol 58:25-45.
631 Martin CB, Douglas D, Newsome RN, Man LL, Barense MD (2018) Integrative and distinctive coding of
632 visual and conceptual object features in the ventral visual stream. Elife 7.
633 Mesulam MM (1998) From sensation to cognition. Brain 121 (Pt 6):1013-1052.
634 Meteyard L, Vigliocco G (2008) 15 - the role of sensory and motor information in semantic
635 representation: A review. In: Handbook of cognitive science (Calvo P, Gomila A, eds), pp 291-
636 312. San Diego: Elsevier.
637 Meyer K, Damasio A (2009) Convergence and divergence in a neural architecture for recognition and
638 memory. Trends Neurosci 32:376-382.

639 Michalka SW, Kong L, Rosen ML, Shinn-Cunningham BG, Somers DC (2015) Short-term memory for space
640 and time flexibly recruit complementary sensory-biased frontal lobe attention networks. Neuron
641 87:882-892.
642 Oldfield RC (1971) The assessment and analysis of handedness: The edinburgh inventory.
643 Neuropsychologia 9:97-113.
644 Padberg J, Seltzer B, Cusick CG (2003) Architectonics and cortical connections of the upper bank of the
645 superior temporal sulcus in the rhesus monkey: An analysis in the tangential plane. J Comp
646 Neurol 467:418-434.
647 Patterson K, Nestor PJ, Rogers TT (2007) Where do you know what you know? The representation of
648 semantic knowledge in the human brain. Nat Rev Neurosci 8:976-987.
649 Petrides M (2005) Lateral prefrontal cortex: Architectonic and functional organization. Philos Trans R Soc
650 Lond B Biol Sci 360:781-795.
651 Romanski LM (2007) Representation and integration of auditory and visual stimuli in the primate ventral
652 lateral prefrontal cortex. Cereb Cortex 17 Suppl 1:i61-69.
653 Sepulcre J, Sabuncu MR, Yeo TB, Liu H, Johnson KA (2012) Stepwise connectivity of the modal cortex
654 reveals the multimodal organization of the human brain. J Neurosci 32:10649-10661.
655 Stuss DT, Benson DF (1986) The frontal lobes. New York: Raven Press.
656 Sugihara T, Diltz MD, Averbeck BB, Romanski LM (2006) Integration of auditory and visual
657 communication information in the primate ventrolateral prefrontal cortex. J Neurosci 26:11138-
658 11147.
659 Thompson-Schill SL, D'Esposito M, Aguirre GK, Farah MJ (1997) Role of left inferior prefrontal cortex in
660 retrieval of semantic knowledge: A reevaluation. Proc Natl Acad Sci U S A 94:14792-14797.
661 Tobyne SM, Osher DE, Michalka SW, Somers DC (2017) Sensory-biased attention networks in human
662 lateral frontal cortex revealed by intrinsic functional connectivity. Neuroimage 162:362-372.

663 Van Hoesen GW, Pandya DN, Butters N (1972) Cortical afferents to the entorhinal cortex of the rhesus

664 monkey. Science 175:1471-1473.

665 Wagner AD, Pare-Blagoev EJ, Clark J, Poldrack RA (2001) Recovering meaning: Left prefrontal cortex

666 guides controlled semantic retrieval. Neuron 31:329-338.

667

668 **Figure Legends**

669

670 **Figure 1**. Schematic illustration of the tasks used in Experiment 1.

671

672 **Figure 2.** Brain areas where similarity between the neural patterns evoked by concepts was
673 significantly correlated with concept similarity according to the semantic model. Results for
674 Experiment 1 (left) and Experiment 2 (right) are shown on dorsal, lateral, medial, and ventral
675 surface views. All results are significant at $p < 0.001$ and cluster corrected at $\alpha < 0.01$. Colors
676 represent t values.

677

678 **Figure 3.** Brain areas where neural similarity was significantly correlated with model similarity in
679 both Experiment 1 and Experiment 2. LACC: left anterior cingulate cortex; LAG: left angular
680 gyrus; LaSTG: left anterior superior temporal gyrus; LdPF: left dorsal prefrontal cortex; LIFG: left
681 inferior frontal gyrus; LIPS: left intraparietal sulcus; LMT: left medial temporal lobe; LMTG: left
682 middle temporal gyrus; LOFC: left orbital frontal cortex; LPCC: left posterior cingulate and
683 precuneus cortex; LSMG: left supramarginal gyrus; LTP: left temporal pole; RAG: right angular
684 gyrus; RaSTG: right anterior superior temporal gyrus; RdPF: right dorsal prefrontal cortex;
685 RIFG: right inferior frontal gyrus; RIns: right insula; RMT: right medial temporal lobe; RMTG:
686 right middle temporal gyrus; ROFC: right orbital frontal cortex; RPCC: right posterior cingulate
687 and precuneus cortex; RSMG: right supramarginal gyrus; RTP: right temporal pole.

688

689 **Figure 4.** Results of hierarchical clustering of neural similarity structures. Left: Dendrogram
690 based on the averaged similarity structures of neural data from 23 ROIs. The vertical axis
691 indicates linkage distance. Right: The 23 ROIs defined by overlapping the RSA maps from the
692 two experiments after thresholding each map at $p < 0.0005$ and cluster-correcting at $\alpha < 0.01$.
693 Anatomical labels match those in Figure 3.

694 **Supplementary Materials**

695

Adjective		Verb		Noun				
aggressive	soft	approached	left	accident	coffee	flower	office	team
angry	spiritual	arrested	liked	activist	commander	football	parent	television
big	tired	ate	listened	actor	company	forest	park	terrorist
black	used	blocked	lived	agreement	computer	girl	party	theater
blue	wealthy	bought	lost	airport	corn	glass	patient	ticket
clever	white	broke	marched	army	council	guard	pencil	tourist
cold	yellow	built	met	artist	couple	hall	pilot	tree
dangerous	young	carried	negotiated	author	court	highway	plane	trial
dark		celebrated	opened	ball	criminal	horse	policeman	vacation
dead		crossed	planned	banker	debate	hospital	politician	victim
dusty		damaged	played	baseball	desk	hotel	priest	voter
empty		delivered	put	beach	dime	hurricane	prison	water
expensive		destroyed	ran	bed	dinner	island	protest	window
famous		drank	read	bicycle	diplomat	journalist	reporter	winter
friendly		drew	saw	bird	doctor	judge	restaurant	witness
green		dropped	shouted	boat	dog	jury	river	woman
happy		ended	slept	book	door	lab	school	worker
heavy		feared	spoke	boy	driver	lake	scientist	
hot		fed	stayed	bread	duck	lawyer	soccer	
injured		fixed	stole	bridge	editor	magazine	soldier	
lonely		flew	survived	businessman	egg	man	spring	
long		found	threw	cabinet	election	mayor	stone	
loud		gave	took	camera	embassy	medicine	store	
new		grew	used	car	engineer	meeting	storm	
old		held	visited	cash	family	minister	street	
peaceful		helped	walked	cellphone	farmer	mob	student	
powerful		hiked	wanted	chair	feather	morning	summer	
red		interviewed	watched	chicken	fence	mountain	sun	
shiny		kicked	went	child	field	mouse	table	
sick		landed	worked	church	fish	newspaper	tea	
small		laughed	wrote	cloud	flood	night	teacher	

696 **Supplementary table**. 1. Words for experiment 1

697

698

Event				Object			
Negative	Nonverbal	Social	Verbal	Animal	Food/Plant	Tool	Vehicle
avalanche	chuckle	bash	lecture	hippopotamus	chestnut	scissors	ferry
battle	squeal	parade	eulogy	fish	ketchup	dime	ambulance
blizzard	screaming	conference	tribute	ant	cranberry	candle	train
bombing	sizzle	rally	deposition	goldfish	flower	stapler	automobile
brawl	screeching	party	showdown	turtle	raspberry	rake	boat
cyclone	applause	tournament	protest	tiger	custard	spatula	bobsled
downpour	siren	gathering	compliment	jackal	sauerkraut	umbrella	skateboard
drought	crescendo	musical	greeting	cricket	mushroom	axe	carriage
earthquake	snap	cruise	testimony	butterfly	pudding	crutches	helicopter
epidemic	growling	wedding	discourse	mosquito	ham	comb	barge
explosion	sneeze	convention	praise	chameleon	honey	tongs	tricycle
famine	boom	circus	rebuke	horse	lemonade	anchor	wagon
flood	thumping	pageant	rebuttal	salmon	tomato	ladle	sled
gunshot	shrieking	luncheon	dispute	alligator	chocolate	sandpaper	motorcycle
gust	sobbing	outing	comment	trout	banana	book	jeep
hail	clattering	jubilee	commemoration	chimpanzee	cider	faucet	van
hailstorm	gulp	expo	denial	chicken	broccoli	pencil	bus
hurricane	whine	reception	trial	duck	pumpkin	glass	plane
inferno	whimpering	banquet	huddle	baboon	bread	hoe	tractor
invasion	melody	reunion	advice	lion	cheese	fork	steamer
landslide	hiccup	dance	quarrel	mouse	champagne	camera	car
lightning	murmuring	feast	thanks	caterpillar	spaghetti	binoculars	rowboat
monsoon	roaring	safari	interrogation	hawk	eggplant	straw	taxi
murder	sigh	celebration	joke	moose	dandelion	calculator	convertible
outbreak	squeaking	fair	plea	snake	egg	stethoscope	streetcar
plague	wheezing	expedition	class	octopus	pineapple	corkscrew	limousine
raid	rumble	concert	recitation	dog	cucumber	cash	glider
riot	bang	symphony	dictation	hamster	milk	handsaw	truck
shooting	giggle	cookout	debate	cardinal	mustard	magazine	rocket
squall	reverberation	contest	sermon	penguin	tobacco	football	canoe
stampede	crackle	carnival	rant	whale	bean	microscope	locomotive
storm	rustle	festival	lesson	crow	jam	hammer	trolley
tempest	thunderclap	housewarming	threat	turkey	blueberry	thermometer	bicycle
thunderstorm	jingle	fiesta	wisecrack	elephant	asparagus	baseball	sleigh
tornado	clapping	march	grievance	bison	nectarine	keyboard	subway
twister	chattering	christening	complaint	cheetah	coffee	key	escalator
volcano	bellowing	prom	apology	rhinoceros	beer	ticket	sailboat
war	grunt	cocktails	commentary	chipmunk	cherry	newspaper	elevator
whirlwind	laughter	picnic	meeting	monkey	plant	hairbrush	submarine
wildfire	groaning	tour	squabble	dolphin	carrot	skillet	scooter

699 **Supplementary table. 2.** Words for experiment 2